Journal of Hazardous Materials 194 (2011) 256–267

Contents lists available at ScienceDirect

Journal of Hazardous Materials

journal homepage: www.elsevier.com/locate/jhazmat

Stabilization of $ZnCl_2$-containing wastes using calcium sulfoaluminate cement: Cement hydration, strength development and volume stability

Stéphane Berger[a], Céline Cau Dit Coumes[a,*], Patrick Le Bescop[b], Denis Damidot[c,d]

[a] Commissariat à l'Energie Atomique et aux Energies Alternatives, CEA/DEN/MAR/DTCD/SPDE, BP17171, 30207 Bagnols-sur-Cèze Cedex, France
[b] Commissariat à l'Energie Atomique et aux Energies Alternatives, CEA/DEN/SAC/DPC/SCCME, 91192 Gif/Yvette, France
[c] University Lille Nord de France, 59000 Lille, France
[d] EM Douai, MPE-GCE, 59508 Douai, France

ARTICLE INFO

Article history:
Received 24 January 2011
Received in revised form 25 July 2011
Accepted 26 July 2011
Available online 5 August 2011

Keywords:
Waste management
Calcium sulfoaluminate cement
Zinc chloride
Hydration
Mechanical strength
Volume stability

ABSTRACT

The potential of calcium sulfoaluminate (CSA) cement was investigated to solidify and stabilize wastes containing large amounts of soluble zinc chloride (a strong inhibitor of Portland cement hydration). Hydration of pastes and mortars prepared with a 0.5 mol/L $ZnCl_2$ mixing solution was characterized over one year as a function of the gypsum content of the binder and the thermal history of the material. Blending the CSA clinker with 20% gypsum enabled its rapid hydration, with only very small delay compared with a reference prepared with pure water. It also improved the compressive strength of the hardened material and significantly reduced its expansion under wet curing. Moreover, the hydrates assemblage was less affected by a thermal treatment at early age simulating the temperature rise and fall occurring in a large-volume drum of cemented waste. Fully hydrated materials contained ettringite, amorphous aluminum hydroxide, strätlingite, together with AFm phases (Kuzel's salt associated with monosulfoaluminate or Friedel's salt depending on the gypsum content of the binder), and possibly C–(A)–S–H. Zinc was readily insolubilized and could not be detected in the pore solution extracted from cement pastes.

1. Introduction

Cementitious materials intended for radioactive waste solidification and stabilization usually include substantial amounts of ordinary Portland cement (OPC) in their formulation. However, wastes produced by nuclear activities are very diverse and some of their components may chemically react with cement phases or mixing water, thus reducing the quality of the product. For instance, ashes resulting from the incineration of technological wastes with neoprene and polyvinylchloride may contain substantial amounts of soluble zinc chloride [1]. This compound is known to have deleterious effects on OPC hydration. Setting is strongly delayed, and can even be inhibited at high zinc loadings [2,3], while hardening is slowed down [4–7]. Moreover, zinc in its ionic form is an environmental pollutant. Acute and chronic effects of zinc have been widely described for different aquatic organisms and exposure routes [8]. In humans, a prolonged and excessive intake of zinc may lead to toxic effects, such as carcinogenesis, mutagenesis and teratogenesis, as a result of its accumulation [9].

The reactivity of Zn(II) in a cementitious system depends both on pH and concentration. At low Zn(II) concentrations (<1 mmol/L), and pH within the range 11.7–12.8, sorption of Zn(II) to calcium silicate hydrate (C–S–H) is observed [10–14]. At high Zn(II) concentrations, the precipitation of β_2-$Zn(OH)_2$ (pH < 12) or calcium zincate $Zn_2Ca(OH)_6{\cdot}2H_2O$ (pH > 12) is observed. The preferential formation of the former [15,16] or latter phase [17–19] on the cement particles has been postulated to explain the delay in cement hydration. Ettringite may also be involved in the retention of Zn(II). By investigating the leaching of cement pastes prepared with a 2 g/L Zn(II) solution, Poon et al. [20] noticed that zinc release and ettringite destabilization occurred simultaneously.

Two approaches may be considered to reduce adverse waste–cement interactions. The first one is to perform a chemical pre-treatment of the waste to convert interfering species to compounds that are stable in cement. Various treatments have been investigated, aiming at precipitating Zn(II) as a phosphate, silicate or calcium compound. The reactions with phosphates and silicates are slow at ambient temperature, and only calcium precipitation would meet industrial requirements [21]. However, the pre-treatment step increases the complexity and cost of the process. The second approach, which is investigated in this article, aims at selecting a binder having improved compatibility with the waste.

Calcium sulfoaluminate (CSA) cements can have highly variable compositions, but all of them contain ye'elimite, also called Klein's compound or tetracalcium trialuminate sulfate, in their

* Corresponding author. Tel.: +33 4 66 39 74 50; fax: +33 4 66 33 90 37.
E-mail address: celine.cau-dit-coumes@cea.fr (C. Cau Dit Coumes).

0304-3894/$ – see front matter © 2011 Elsevier B.V. All rights reserved.
doi:10.1016/j.jhazmat.2011.07.095

Table 1
Mineralogical composition of the investigated CSA clinker (KTS 100 provided by Belitex).

Minerals	$C_4A_3\underline{S}$	C_2S	$C_{12}A_7$	CT	Periclase	$C\underline{S}$	Quartz	Others[a]
wt%	68.5	15.9	9.5	2.9	1.5	0.5	0.5	2.4

[a] Include 1.2% of iron oxide.

clinker [22–25]. In this article, we will consider only sulfoaluminate belite cements in which ye'elimite ($C_4A_3\underline{S}$[1]) predominates over belite (C_2S) [26]. A wide range of gypsum contents (typically from 10 to 25%) can be ground with CSA clinker to produce different CSA cements, ranging from rapid-hardening (at low gypsum content) to shrinkage-compensating, and eventually to self-stressing (at high gypsum content) [27]. The hydration progress of CSA cement pastes occurs by the initial precipitation of ettringite and aluminum hydroxide, followed by the precipitation of calcium monosulfoaluminate hydrate once calcium sulfate has been depleted [28–30]. The contents of ettringite and calcium monosulfoaluminate hydrate are very sensitive to the amount of added sulfate: the former dominates in a gypsum-rich environment, whereas the latter tends to increase in a gypsum-deficient system [31]. Depending on the composition of the minor phases, other hydration products may also precipitate, such as C–S–H [28,32], strätlingite [33–35], siliceous hydrogarnet [34] and/or hemi- or monocarboaluminate [36].

CSA cements may present at least two advantages to stabilize $ZnCl_2$-rich wastes. Their hydration is much less retarded by zinc chloride than that of OPC [37]. Moreover, their two main hydrates, ettringite and calcium monosulfoaluminate hydrate, are expected to provide good Zn^{2+} confinement due to their flexible structure [38–44].

This work aimed at assessing the potential of CSA cement to stabilize wastes with high contents of soluble zinc chloride. A cement matrix material intended for immobilisation has to meet a number of requirements. The cemented waste form should set within a reasonable period of time and remain a stable monolith thereafter. Excessive heat generation during hydration should be avoided, as well as segregation of water. Moreover, the pollutants from the waste should be insolubilized. This work had thus three main issues:

- supplement the data concerning hydration at early age of CSA cements by a $ZnCl_2$ solution by following their mineralogical evolution over one year,
- assess the influence on hydration of a brief temperature rise and fall at early age, as it may occur in a 200 L drum filled with a cemented waste,
- investigate the strength development and volume change of $ZnCl_2$-rich mortars as a function of their gypsum content.

2. Experimental

2.1. Materials and specimen preparation

CSA cements were prepared by mixing a ground industrial CSA clinker (composition in Table 1; d_{10} = 2.67 μm, d_{50} = 17.6 μm, d_{90} = 50.8 μm, BET specific surface area = 1.3 m^2/g) with the appropriate amount of analytical grade gypsum (from 0 to 20% by weight of cement; d_{10} = 5.4 μm, d_{50} = 19.6 μm, d_{90} = 50.3 μm, BET specific surface area = 0.4 m^2/g) for 15 min. In the clinker, ye'elimite predominated over belite and mayenite. The other minor constituents, mainly phases containing titanium and iron, could be regarded as hydraulically inactive. Both cement pastes and mortars were made with the same w/c ratio of 0.55 for an easier comparison of their hydration rate. The selected ratio (0.55) resulted from a compromise. It enabled the preparation of mortars with an acceptable workability, while the corresponding cement pastes did not exhibit any bleeding. Moreover, the water content was slightly higher than the chemical water demand of the binder comprising 80% clinker and 20% gypsum, as assessed in a previous work [47] (water demand corresponding to a w/c ratio of 0.54). A blend of two siliceous sands (0.1–1.2 mm), with a sand to cement weight ratio of 3, was used to optimize the workability and limit the heat release of fresh mortars during hydration. The mixing solution was prepared by dissolving analytical grade salt into distilled water ($ZnCl_2$ 0 or 0.5 mol/L, which was representative of the concentration released in mixing water by actual incinerator ashes). Mixing was performed in a standardized laboratory mixer (following European standard EN 196-1) at low speed for 3 min and at high speed for 2 min. Cement pastes were cast into airtight polypropylene boxes (7 mL of paste per box), and cured at 20 °C for one year, or submitted to a thermal treatment in an oven (Memmert UFP500) for 7 d before being cured at 20 °C. Mortars were cast into 4 cm × 4 cm × 16 cm moulds and cured for 7 d at 20 ± 1 °C and 95 ± 5% R.H., or submitted to a thermal treatment. The specimens were then demoulded, weighed, measured, and kept at room temperature in sealed bag or immersed under water at 20 ± 1 °C. Mortars were also used for semi-adiabatic calorimetry investigation.

Shorthand notations were used to refer to the different investigated compositions, as summarized in Table 2.

Complementary experiments were performed on cement suspensions (w/c ratio = 10) stirred under nitrogen atmosphere at room temperature for 7 d. The objective was to reach higher degrees of hydration than in cement pastes.

2.2. Thermal cycles

Thermal cycles were applied on pastes and mortars just after mixing with the objective to reproduce the temperature rise and fall occurring in a massive mortar block. In a preliminary study, it was shown that the temperature evolution in the heart of a 200 L metallic drum filled with a cemented waste (mortar with typical w/c and s/c ratios of 0.55 and 3) could be reasonably well assessed by recording the temperature during hydration of 800 mL of the same mortar sample placed in a semi-adiabatic Langavant calorimeter. Such curves were thus recorded for each investigated cement composition (Fig. 1). Temperature profiles were then defined by interpolating the curves as closely as possible. Since cement pastes produced more heat than mortars, some corrections were implemented when necessary to keep similar temperature evolutions in the heart of mortars and their corresponding pastes with the same gypsum content.

2.3. Characterization methods

Hydration of mortars was followed by calorimetry according to the semi-adiabatic method (European standard EN 196-9). This latter consisted in introducing 1575 ± 1 g of fresh mortar into a cylindrical container, which was then placed into a calibrated Langavant calorimeter to determine the quantity of heat emitted versus the temperature evolution.

[1] Shorthand cement notations are used in this article: C = CaO, S = SiO_2, $\underline{S}$ = SO_3, A = Al_2O_3, H = H_2O, T = TiO_2.

Table 2
Shorthand notations of the investigated compositions.

Gypsum content (% by weight of cement)	$[ZnCl_2]$ in mixing water (mol/L)	Paste		Mortar	
		Curing at 20 °C	Thermal treatment at early age	Curing at 20 °C	Thermal treatment at early age
0	0	CE0	CE0t	ME0	ME0t
	0.5	CZ0	CZ0t	MZ0	MZ0t
20	0	CE2	CE2t	ME2	ME2t
	0.5	CZ2	CZ2t	MZ2	MZ2t

The core temperature of pastes and mortars was measured with waterproof penetration probes (type K TC) and recorded with a Testo 735-2 thermometer.

Hydration was stopped after fixed periods of time (from 5 min to 1 year) by successively immersing the crushed pastes into isopropanol and drying them in a controlled humidity chamber (with 20% relative humidity at 22 ± 2 °C).

Crystallized phases were identified by X-ray diffraction (Siemens D8 – copper anode $\lambda_{K\alpha1}$ = 1.54056 Å generated at 40 mA and 40 kV) on pastes and mortars ground to a particle size of less than 100 μm. Concerning mortars, the samples were first crushed coarsely and a part of the sand grains was removed by sieving at 200 μm before the grinding step to a particle size below 100 μm. The acquisition range was from 5° to 60° 2θ in 0.02° 2θ steps with integration at the rate of 50 s per step. The evolution of the amounts of reactants and products over time was qualitatively assessed from XRD patterns by measuring the areas of corresponding reflections using the EVA software (© 2005 Bruker AXS). Thermogravimetric analyses were carried out under nitrogen on 50 ± 2 mg of sample using a TGA/DSC Netzsch STA409 PC instrument at 10 °C/min up to 1000 °C.

The compressive strength of mortar prisms cured in sealed bag or under water was measured following European standard EN 196-1 after 1 d, 7 d, 28 d, 90 d, 180 d and 360 d. Triplicate specimens were used at each testing age.

Expansion under water was assessed on mortar bars placed into cells filled with 700 mL of demineralised water (one sample per cell). Their length change was measured with displacement gauges (linear variable differential transducers, measurement range ±1 mm, resolution 1 μm). A sketch of the device is given in [45]. Measurements were recorded every hour over approximately one year, which allowed an accurate monitoring of the samples evolution. Mass gain was assessed on additional specimens kept under water at room temperature after 7 d, 28 d, 90 d, 180 d and 360 d.

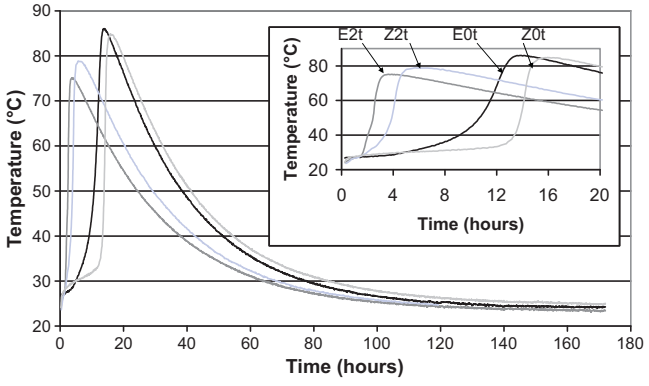

Fig. 1. Thermal cycles applied to pastes and mortars as a function of the initial gypsum content of the cement (0, 0% gypsum; 2, 20% gypsum) and zinc concentration (E, 0 mol/L; Z, 0.5 mol/L) in the mixing solution.

Total water porosity Φ_w was estimated by measuring the total water amount removed from water-saturated mortar samples after drying at 60 °C (to limit ettringite degradation) until stable mass loss (Eq. (1)).

$$\Phi_w\ (\%) = \frac{m_a - m_d}{m_a - m_w} \times 100 \quad (1)$$

where m_a and m_w are the water-saturated sample mass values measured in air and under water, respectively, and m_d the mass of the dried sample measured in air.

The pore solution composition of cement pastes was determined by extracting their interstitial solution using high pressure. A crushed sample (≈300 g) was placed in the cavity of the pore pressing device. Pressure was then applied to the piston at a rate of 20 MPa/min, with plateaux at 110, 225 and 340 MPa, until a maximum load pressure of 450 MPa (Walter Bai 102/3000-HK4). The pore solution was collected in a plastic tube maintained in slight depression. At the end of the experiment the sampling tube was transferred into a N_2 glovebox, and the collected solution was filtered at 0.2 μm before analysis by ICP-AES.

Thermodynamic calculations were carried out using the CHESS software [46]. The solubility constants of CSA cement hydrates were previously given in [47], those of the Kuzel's and Friedel's salts were taken from [48]. The data relative to zinc-containing phases are summarized in Table 3.

3. Results

3.1. Rate of hydration

The rate of hydration of the cement pastes prepared with a 0.5 mol/L $ZnCl_2$ solution was investigated as a function of their gypsum content. The core temperature of the materials either cured at 20 °C or in a semi-adiabatic Langavant calorimeter was recorded versus time, and the residual ye'elimite content of the pastes was assessed from their XRD patterns (Fig. 2). Hydration of the gypsum-free cement at room temperature was retarded by almost 70 h compared with a reference prepared with pure water (Fig. 2a). After 1 d, only 18% of ye'elimite were depleted, versus 83% for the reference. Simulating a temperature rise up to 85 °C strongly reduced the hydration delay. The heat flux reached its maximum after 14.3 h, instead of 12.1 h for the reference with pure water cured under the same conditions, and ye'elimite was almost fully consumed after 24 h (residual of 2%) (Fig. 2b). Raising the gypsum content of the binder to 20% was another way to increase the rate of hydration. The maximum temperature was reached after 8.3 h in sample CZ2, instead of 79 h for sample CZ0 (Fig. 2a and c). Similarly, with a thermal cycle, the heat flux reached its maximum after 3.2 h in sample CZ2t instead of 14.3 h in sample CZ0t (Fig. 2d). With 20% gypsum, the retardation induced by zinc chloride was almost suppressed: pastes CE2 and CZ2 exhibited rather similar ye'elimite depletion rates (Fig. 2c). The origin of the retardation induced by $ZnCl_2$ on gypsum-free CSA cement was discussed in a previous work [37]. Unlike what would be expected for OPC, the delay results from the

Table 3
Solubility data (T = 25 °C, 1 bar) of the zinc-containing phases considered for thermodynamic modelling.

Mineral	Formation reaction	Log K
$CaZn_2(OH)_6$	$Ca^{2+} + 2Zn^{2+} + 6H_2O \rightarrow CaZn_2(OH)_6 + 6H^+$	−44.56
$Zn_2(OH)_3Cl$	$2Zn^{2+} + Cl^- + 3H_2O \rightarrow Zn_2(OH)_3Cl + 3H^+$	−15.2921
$Zn_5(OH)_8Cl_2$	$5Zn^{2+} + 2Cl^- + 8H_2O \rightarrow Zn_5(OH)_8Cl_2 + 8H^+$	−38.5000
$ZnCl_2$	$Zn^{2+} + 2Cl^- \rightarrow ZnCl_2$	−7.088
Zincite	$Zn^{2+} + H_2O \rightarrow ZnO + 2H^+$	−11.2087
$Zn(OH)_2$ (beta)	$Zn^{2+} + 2H_2O \rightarrow Zn(OH)_{2\ beta} + 2H^+$	−11.9341
$Zn(OH)_2$ (epsilon)	$Zn^{2+} + 2H_2O \rightarrow Zn(OH)_{2\ epsilon} + 2H^+$	−11.6625
$Zn(OH)_2$ (gamma)	$Zn^{2+} + 2H_2O \rightarrow Zn(OH)_{2\ gamma} + 2H^+$	−11.8832
$ZnSO_4{\cdot}7H_2O$	$Zn^{2+} + SO_4^{2-} + 7H_2O \rightarrow ZnSO_4{\cdot}7H_2O$	1.8683
$ZnSO_4{\cdot}6H_2O$	$Zn^{2+} + SO_4^{2-} + 6H_2O \rightarrow ZnSO_4{\cdot}6H_2O$	1.6846
$ZnSO_4{\cdot}H_2O$	$Zn^{2+} + SO_4^{2-} + H_2O \rightarrow ZnSO_4{\cdot}H_2O$	0.5383
$ZnSO_4$	$Zn^{2+} + SO_4^{2-} \rightarrow ZnSO_4$	−3.5425
$Zn_2SO_4(OH)_2$	$2Zn^{2+} + SO_4^{2-} + 2H_2O \rightarrow Zn_2SO_4(OH)_2 + 2H^+$	−7.5816
$Zn_3O(SO_4)_2$	$3Zn^{2+} + 2SO_4^{2-} + H_2O \rightarrow Zn_3O(SO_4)_2 + 2H^+$	−19.1188
$Zn_4(OH)_6SO_4$	$4Zn^{2+} + SO_4^{2-} + 6H_2O \rightarrow Zn_4(OH)_6SO_4 + 6H_2O$	−28.4000

Data from the Minteq database [52] and from [53].

strong retardation caused by chloride anions, which is partly balanced by an accelerating effect due to zinc cations. Sulfates also strongly accelerate hydration and, when gypsum is added to the binder at a level of 20%, the delay is almost compensated.

3.2. Mineralogical evolution over one year

The mineralogical changes of the cement pastes with ongoing hydration were determined by XRD and TGA (Figs. 3–7). Fig. 8 summarizes the evolution over time of the hydrate assemblage in the four investigated materials (CZ0, CZ0t, CZ2, CZ2t).

3.2.1. Paste CZ0

During the first 5 min of hydration, a rapid stiffening of the paste occurred simultaneously with the precipitation of gypsum and of an unidentified compound, subsequently referred to as "phase λ", which was responsible for two diffraction peaks at 2θ = 7.8° (most intense) and 15.7°, and for weight losses at 95 °C and 195 °C by TGA. SEM observations of the paste showed the formation of crystals with platelet morphology, which were too fine to be analysed by EDX (Fig. 9). Up to 24 h, only small amounts of hydrates precipitated, mainly ettringite, which replaced gypsum, phase λ, amorphous aluminum hydroxide (AH_3), and Friedel's salt, an AFm phase in which the positively

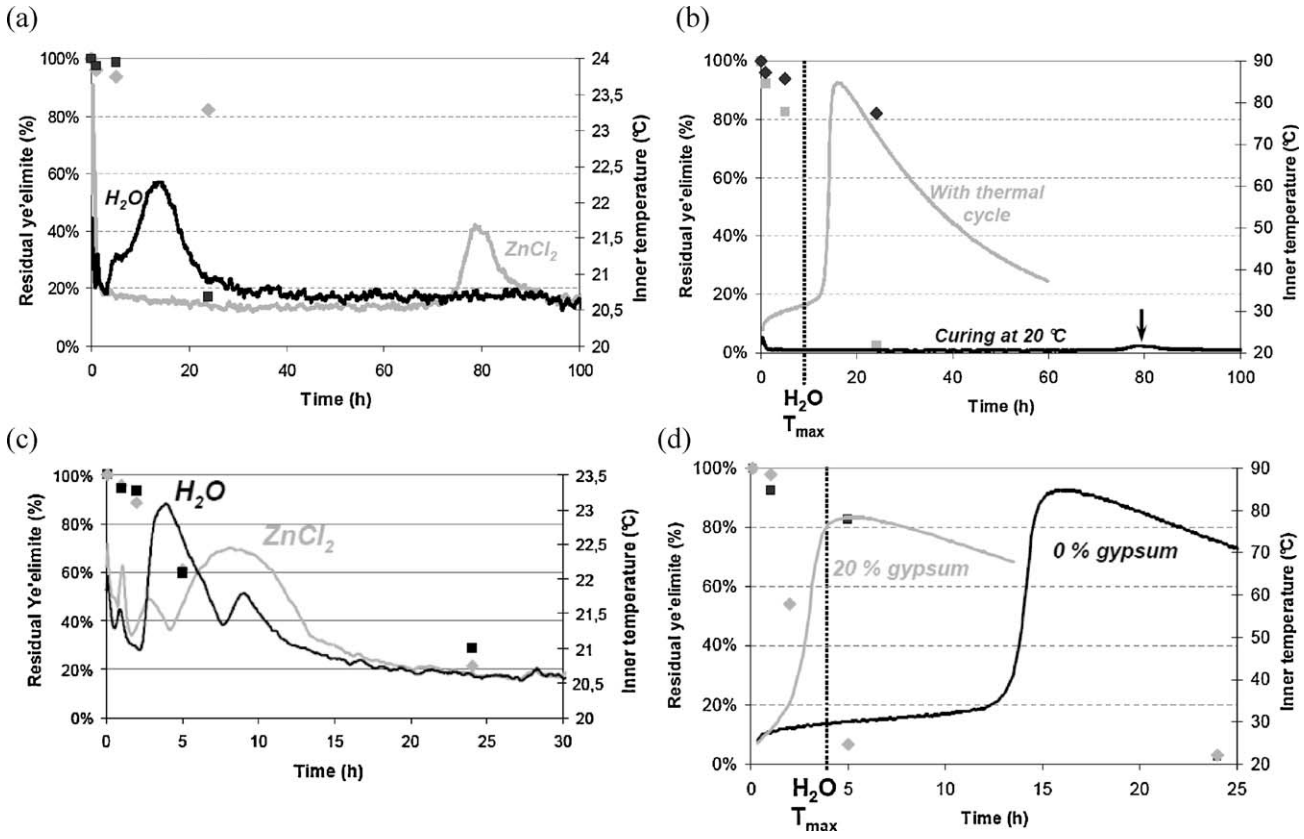

Fig. 2. Influence of the composition of the mixing water, gypsum content of the binder and curing conditions on the hydration rate of CSA cements (dots, ye'elimite content; curves, temperature). (a) Gypsum = 0%; curing at 20 °C; mixing solution = water or ZnCl2 0.5 mol/L. (b) Gypsum = 0%; curing at 20 °C or thermal treatment; mixing solution = $ZnCl_2$ 0.5 mol/L. (c) Gypsum = 20%; curing at 20 °C; mixing solution = water or $ZnCl_2$ 0.5 mol/L. (d) Gypsum = 0% or 20%; thermal treatment; mixing solution = $ZnCl_2$ 0.5 mol/L.

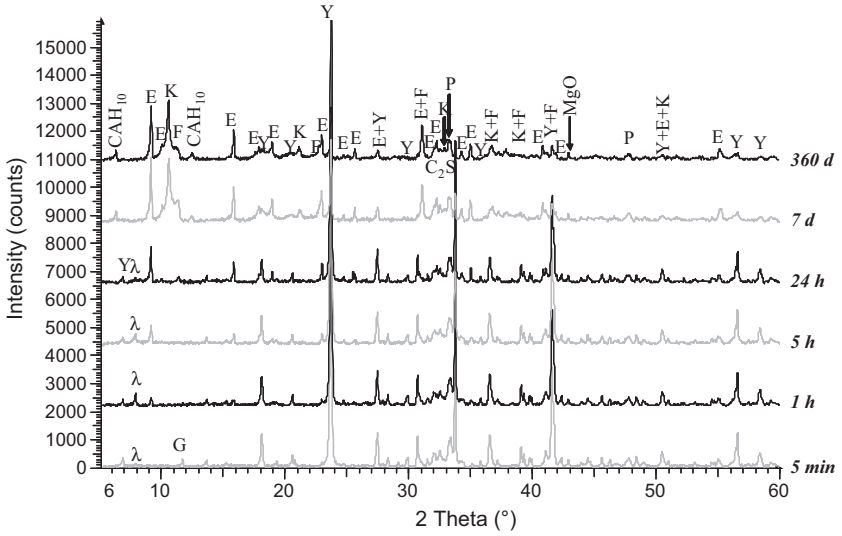

Fig. 3. X-ray diffraction analysis of cement paste CZ0 cured at 20 °C after 5 min, 1 h, 5 h, 24 h, 7 d, and one year of hydration. E, ettringite; F, Friedel's salt; K, Kuzel's salt; Y, ye'elimite; P, perovskite; G, gypsum.

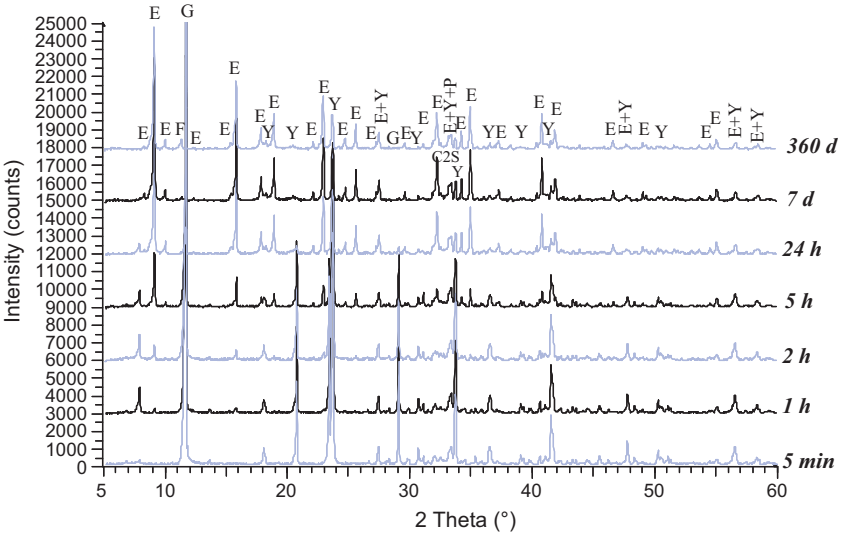

Fig. 4. X-ray diffraction analysis of cement paste CZ2 cured at 20 °C after 5 min, 1 h, 2 h, 5 h, 24 h, 7 d, and one year of hydration. E, ettringite; F, Friedel's salt; Y, ye'elimite; P, perovskite; G, gypsum.

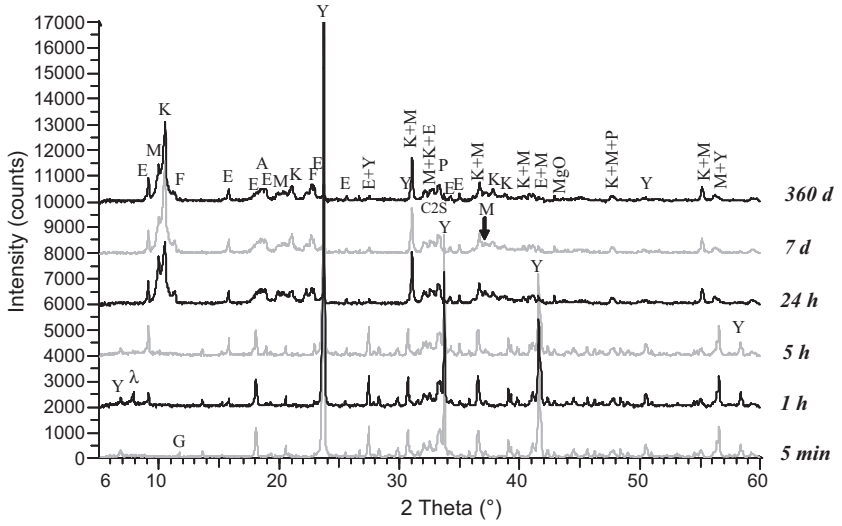

Fig. 5. X-ray diffraction analysis of cement paste CZ0t cured at 20 °C after 5 min, 1 h, 5 h, 24 h, 7 d, and one year of hydration. E, ettringite; F, Friedel's salt; K, Kuzel's salt; M, calcium monosulfoaluminate hydrate; Y, ye'elimite; P, perovskite; G, gypsum.

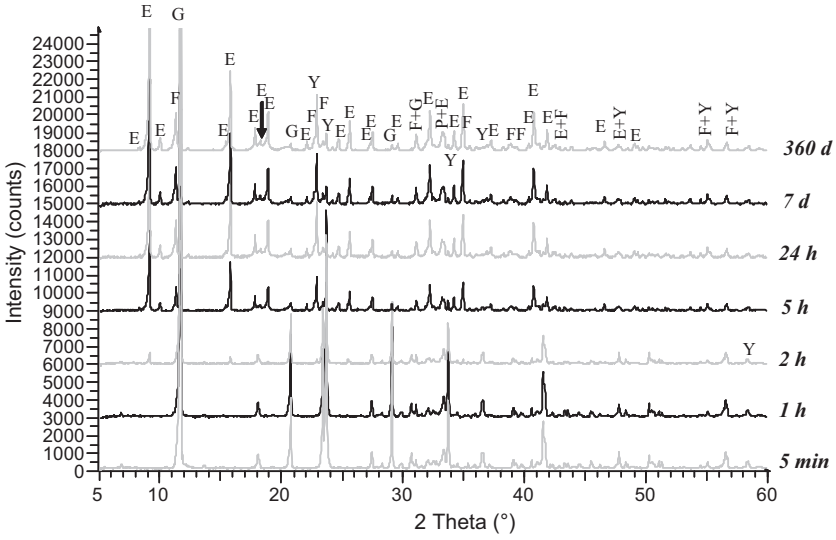

Fig. 6. X-ray diffraction analysis of cement paste CZ2t cured at 20 °C after 5 min, 1 h, 2 h, 5 h, 24 h, 7 d, and one year of hydration. E, ettringite; F, Friedel's salt; Y, ye'elimite; P, perovskite; G, gypsum.

charged main layers are balanced by the insertion of chloride anions in the interlayer ($C_3A{\cdot}CaCl_2{\cdot}10H_2O$). After 7 d, phase λ was no longer detected and the phase assemblage had significantly evolved. The main hydrates were ettringite and Kuzel's salt, an AFm-structured compound containing ordered chloride and sulfate anions ($C_3A{\cdot}1/2CaSO_4{\cdot}1/2CaCl_2{\cdot}10H_2O$). Smaller amounts of CAH_{10}, monosulfoaluminate and Friedel's salt were also observed. At later age, from 7 d to 1 year, the paste exhibited only minor mineralogical evolutions. The residual amount of ye'elimite slightly decreased (from 13% to 7%) while the amount of Kuzel's salt tended to increase at the expense of Friedel's salt. CAH_{10} is usually known to be formed mainly at low temperature (below 15 °C) during the hydration of calcium aluminate cement. However, its formation has already been reported at 20–25 °C during the hydration of CSA clinker [37,49]. Nevertheless, CAH_{10} is a metastable phase at ambient temperature and is expected to be transformed at later

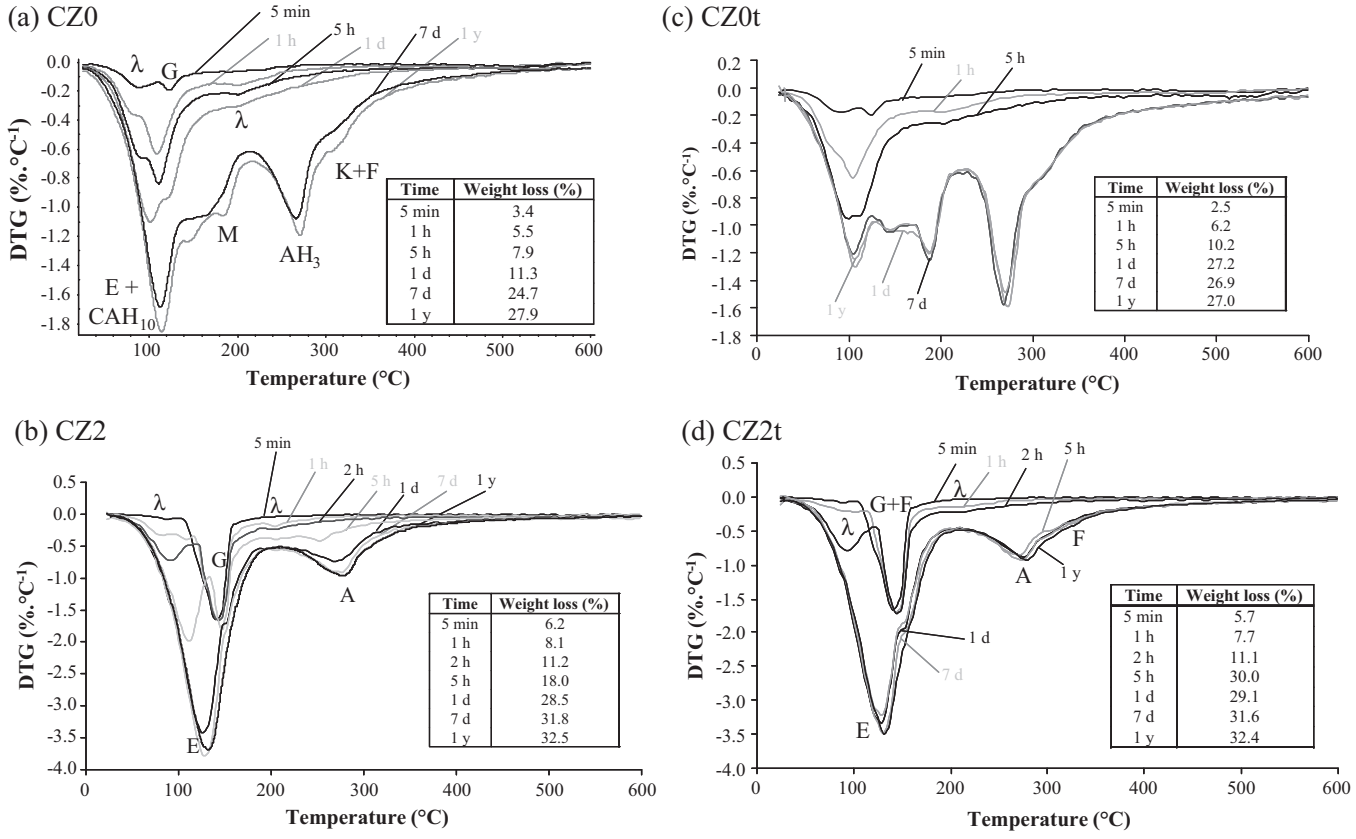

Fig. 7. Thermogravimetry analysis of cement pastes CZ0 (a), CZ2 (b), CZ0t (c) and CZ2t (d) after increasing periods of hydration. E, ettringite; G, gypsum; A, aluminum hydroxide; M, calcium monosulfoaluminate hydrate; K, Kuzel's salt; F, Friedel's salt.

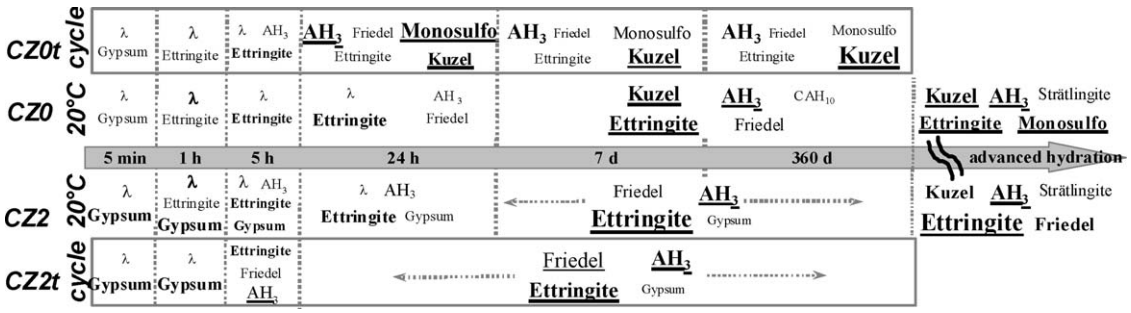

Fig. 8. Comparison of the hydrated phase assemblage in samples CZ0, CZ0t, CZ2 and CZ2t with ongoing hydration (curing at 20 °C or with a thermal treatment (cycle); advanced hydration obtained by hydration with excess water (w/c = 10) under stirring at 20 °C for 7 d).

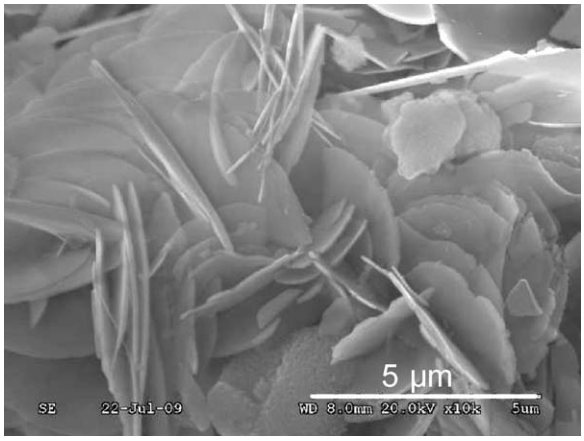

Fig. 9. SEM observation of phase λ in paste CZ0 after 5 min of hydration.

age. To assess the long term evolution of paste CZ0, the cement was hydrated using the suspension technique (w/c = 10) with the same [$ZnCl_2$]/cement ratio as in the cement paste (the $ZnCl_2$ concentration in the solution was thus decreased to 0.0275 mol/L to take into account the dilution factor of the suspension). After one week of mixing, the reactive anhydrous phases of the clinker (ye'elimite and mayenite) were totally depleted. The water loss determined by TGA reached 32%, which corresponded to a w/c ratio of 0.47. The chemical water demand of the clinker was thus lower than the investigated w/c ratio (0.55). The phase assemblage comprised monosulfoaluminate and Kuzel's salt, ettringite, AH_3 and strätlingite (Fig. 10). Crystallized Zn-containing phases were not detected. In addition to the precipitation of Cl-AFm phases, the CSA clinker hydrated with a $ZnCl_2$ solution differed from a reference prepared with pure water by its higher ettringite content, and lower strätlingite content. As chloride ions partly replaced sulfates in the structure of the AFm phases, more sulfates were available for ettringite precipitation in CZ0 than in CE0. Precipitation of strätlingite is well predicted by thermodynamic calculations simulating the addition of belite to a phase assemblage resulting from the hydration of ye'elimite [34,47]. Strätlingite is formed according to balance equation $C_2S + AH_3 + 5H \rightarrow C_2ASH_8$ as long as AH_3 is present in the system. Precipitation of C–S–H requires an excess of belite over ye'elimite. Two assumptions may be considered to explain the low content of strätlingite in suspension CZ0:

- the local precipitation of C–S–H near C_2S grains could not be excluded,
- or more likely, belite was not fully reacted, its hydration being strongly delayed by zinc chloride.

3.2.2. Paste CZ0t

The temperature in paste CZ0t exceeded 70 °C from 14 to 26 h. As already observed for CSA cement pastes prepared with pure water [37], high temperatures promoted the precipitation of monosulfoaluminate instead of ettringite, which had a smaller stability domain under these conditions [50]. After 1 d, the amount of monosulfoaluminate tended to decrease, together with that of Friedel's salt, to form Kuzel's salt. This evolution was consistent with the results of Glasser et al. [51] and Balonis et al. [48], showing that the binary monosulfoaluminate/Friedel's salt system is unstable and leads to

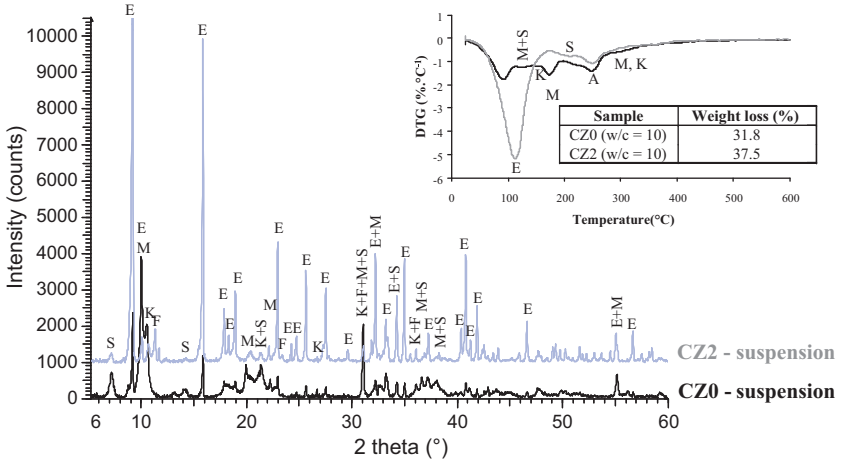

Fig. 10. X-ray diffraction and thermogravimetry analysis of cement suspensions prepared from CZ0 and CZ2 (w/c ratio increased to 10, constant Zn/c ratio) after one week of stirring at 20 °C under nitrogen atmosphere. E, ettringite; F, Friedel's salt; K, Kuzel's salt; M, calcium monosulfoaluminate hydrate; S, strätlingite; A, AH3.

the formation of Kuzel's salt and monosulfoaluminate (respectively Friedel's salt) if the $[SO_4]/[Cl_2]$ ratio is above (respectively below) 1. The temperature rise also induced a faster consumption of phase λ, which could no longer be detected beyond 5 h (instead of 24 h for the paste cured at room temperature), and CAH_{10} was never observed (whereas it persisted from 7 d to 1 year in paste CZ0).

3.2.3. Paste CZ2

When the CSA clinker was blended with 20% gypsum, precipitation of phase λ at early age increased. However, this compound could not be detected beyond 1 d. The main hydrates were then ettringite and AH_3. The gypsum addition clearly promoted the precipitation of AFt instead of AFm phases as already observed for pastes prepared with pure water [47]. Only small amounts of Friedel's salt were detected after 7 d, and increased slightly over one year, meaning that a significant fraction of chlorides should remain insolubilized. The pore solutions of 1 d, 7 d, and 28 d old cement pastes (w/c raised to 0.75 to collect enough solution) were extracted using pressure, and analysed (Table 4). As expected, their chloride concentrations were important, ranging from 150 to 250 mmol/L, and counterbalanced by high concentrations of calcium, sodium and potassium. Conversely, their zinc concentration always remained below the detection limit (<2 μmol/L). The long-term evolution of cement paste CZ2 was assessed from the analysis of a cement suspension (w/c = 10, $[ZnCl_2]$ = 0.0275 mol/L in the solution to maintain a constant $[ZnCl_2]$ to [cement] ratio). After one week of stirring at room temperature, ye'elimite and mayenite were totally consumed. The precipitated hydrates were mainly ettringite and AH_3, with smaller amounts of strätlingite, Friedel's and Kuzel's salts (Fig. 10). For comparison, the hydrate assemblage of a reference prepared with pure water contained ettringite, AH_3, strätlingite and monosulfoaluminate which formed once gypsum was depleted. In the presence of $ZnCl_2$, monosulfoaluminate was replaced by the Kuzel's salt given the instability of the monosulfoaluminate/Friedel's salt system.

3.2.4. Paste CZ2t

Paste CZ2t exhibited very rapid hydration. After only 5 h, gypsum was almost totally consumed and the residual ye'elimite content reached 7%. Phase λ briefly precipitated at early age, but was rapidly depleted: it was no longer detected after 2 h. The hydrates assemblage observed from 5 h to one year comprised ettringite, Friedel's salt and AH_3. Friedel's salt was precipitated in much higher amounts than in the paste cured at 20 °C, while the ettringite content was slightly lower. With rising temperature, there was a drop in the thermodynamic stability of ettringite in favour of Friedel's salt. However, with the subsequent decrease in temperature, ettringite could form again at the expense of Friedel's salt: between 7 d and one year, the X-ray diffraction patterns showed a slight increase in the ettringite peaks, and a decrease in those corresponding to Friedel's salt.

3.2.5. Modelling of the mineralogical evolution

The chronological evolutions of the phases precipitated during hydration in pastes CZ0 and CZ2 were in fairly good agreement (excepting the Zn-containing phases) with thermodynamic calculations simulating the hydration of ye'elimite, or ye'elimite + gypsum, in a $ZnCl_2$ solution. Fig. 11a shows for instance the modelling of the progressive hydration of ye'elimite in sample CZ0 with a w/c ratio of 10 (corresponding to the suspension experiment). The calculation predicted the successive precipitation of AH_3, ettringite (pH > 10), Friedel's salt (pH > 11.5), Kuzel's salt (pH > 11.8) with consumption of Friedel's salt, and finally monosulfoaluminate. The final phase assemblage (AH_3, ettringite, Kuzel's salt and monosulfoaluminate) was in good agreement with the experiment (see Fig. 10). The same calculation performed at a lower w/c ratio, such as in the cement paste, showed that, in the very first stages of hydration, the system was also oversaturated with respect to gypsum. Gypsum was actually observed in paste CZ0 5 min after the beginning of hydration. Simulating the complete hydration of ye'elimite in sample CZ2 at a w/c ratio of 10 led to the total

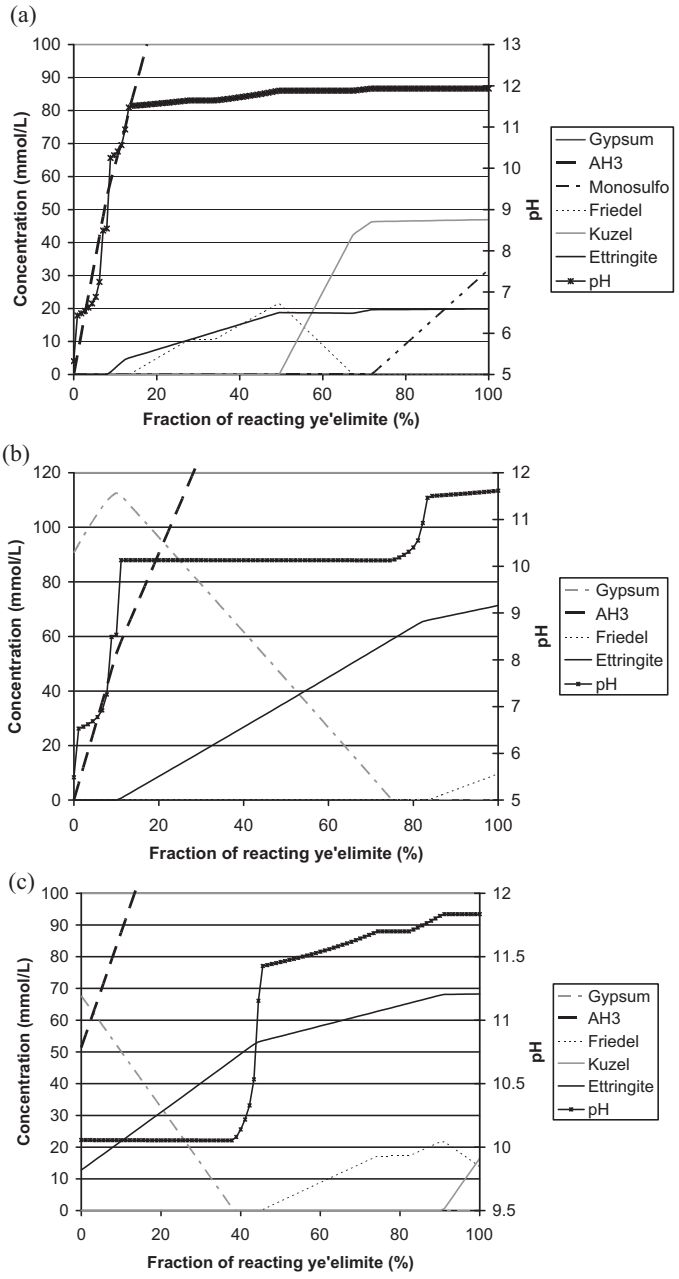

Fig. 11. Thermodynamic modelling of the hydrates assemblage with ongoing hydration. (a) Dissolution of ye'elimite (from 0 to 113 mmol/L) in a solution containing initially 27.5 mmol/L of Zn^{2+} and 55 mmol/L of Cl^- (simulation of the progressive hydration of ye'elimite in sample CZ0 with a w/c ratio of 10). (b) Dissolution of ye'elimite (from 0 to 90 mmol/L) in a suspension containing initially 27.5 mmol/L of Zn^{2+}, 55 mmol/L of Cl^- and 116.2 mmol/L of gypsum (simulation of the progressive hydration of ye'elimite in sample CZ2 with a w/c ratio of 10). (c) Dissolution of ye'elimite (from 0 to 90 mmol/L) in a suspension containing initially 27.5 mmol/L of Zn^{2+}, 55 mmol/L of Cl^-, 116.2 mmol/L of gypsum and 5.5 mmol/L of $C_{12}A_7$ (simulation of the progressive hydration of ye'elimite in sample CZ2 with a w/c ratio of 10 – mayenite is considered as fully hydrated). The zinc-containing phases were omitted for better clarity. The model predicted the successive precipitation of simonkolleite ($Zn_5(OH)_2Cl_2$) (pH ≤ 8.5), $Zn(OH)_5$ (8.5 ≤ pH ≤ 11.7), and hydroxyzincate ($CaZn_2(OH)_6$) (pH ≥ 11.7). Zincite (ZnO) is more stable than zinc hydroxide, but is known to precipitate with a slower rate. It was thus excluded from the database.

Table 4
Composition of the pore solutions extracted from pastes CE2 and CZ2 (w/c = 0.75) cured for 1 d, 7 d and 28 d at 20 °C and 95% R.H. (total concentrations in mmol/L, conductivity in mS).

	CE2			CZ2		
	1 d	7 d	28 d	1 d	7 d	28 d
Zn^{2+}	–	–	–	<0.002	<0.002	<0.002
K^+	53	55	52	82	90	97
Na^+	21	15	5.5	60	59	32
Ca^{2+}	0.47	0.25	0.20	250	140	82
Sr^{2+}[a]	<0.001	<0.001	<0.001	7.6	4.8	3.8
Al^{3+}	12	7.6	6.9	<0.001	<0.001	<0.001
Cl^-	7	5	4	250	190	150
SO_4^{2-}	1.3	0.82	2.4	0.89	0.44	0.77
pH	12.3	12.4	12.3	9.8	9.6	9.5
Conductivity	8.2	11	9.2	49	37	32

[a] Strontium was initially contained by the clinker (0.09 wt%).

consumption of gypsum, and to the precipitation of AH_3, ettringite and Friedel's salt (Fig. 11b). In the suspension experiment, small amounts of Kuzel's salt were also noticed (Fig. 10). Precipitation of Kuzel's salt could be reproduced by the model by taking into account the full hydration of mayenite, in addition to ye'elimite (Fig. 11c).

For both systems (CZ0 and CZ2), the calculations overestimated the amount of AH_3 precipitated at the beginning of hydration. In the cement pastes, the latter may have been limited by the incorporation of aluminum in transient phase λ.

3.3. Compressive strength

The properties of hardened materials were investigated on heat-treated mortars MZ0t and MZ2t to take into account the significant temperature rise occurring in actual cemented waste drums as a result of the heat generated by hydration. Fig. 12 shows the evolution with time of their compressive strength, which increased very rapidly. It already reached 89 ± 5% of the one-year strength after 1 d, compared with 79 ± 9% for mortars ME0t and ME2t prepared with pure water. Hardening was thus accelerated by zinc chloride. The compressive strength continued to increase at later age, but much more slowly. This result is consistent with the rapid hydration of the binders, which exhibited only small mineralogical evolutions beyond 1 d. Zinc chloride also improved the one-year strength of the mortars, especially when the cement contained gypsum (increase of 31 ± 7% for MZ2t compared to ME2t, and 13 ± 5% for MZ0t compared to ME0t). These results could not be simply explained by differences in the total water porosity of the samples. For instance, mortars MZ2t and ME2t had almost the same total porosity, but exhibited very different compressive strengths.

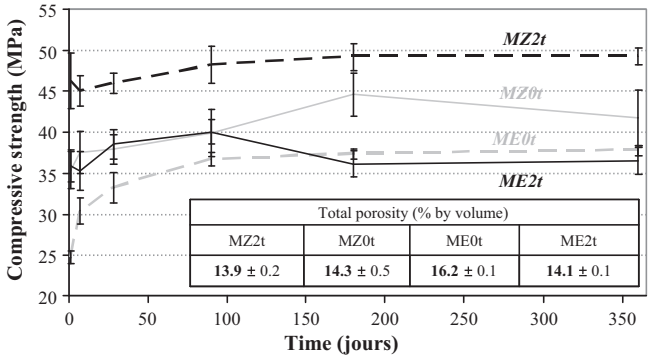

Fig. 12. Compressive strength and water porosity of 4 cm × 4 cm × 16 cm mortar specimens submitted to a thermal treatment at early age, and subsequently cured in sealed bag at room temperature.

Possible modifications of the ITZ might be involved, as well as differences in the pore distribution. Preliminary attempts to characterize this distribution using mercury intrusion porosimetry were not successful. The total porosities measured with this technique were unexpectedly high. We suspected that the high vacuum required by the method damaged ettringite due to a strong dehydration, and thus modified the microstructure.

3.4. Volume stability under water

The length change and mass gain of the mortars cured under water are summarized in Fig. 13. The samples were immersed after 7 d and exhibited a rapid mass increase which may have had different origins: water uptake due to capillary suction to compensate for water depleted by hydration, water penetration due to osmosis (the interstitial solution being more concentrated than the curing solution), and continued hydration. The mass gain was rapid

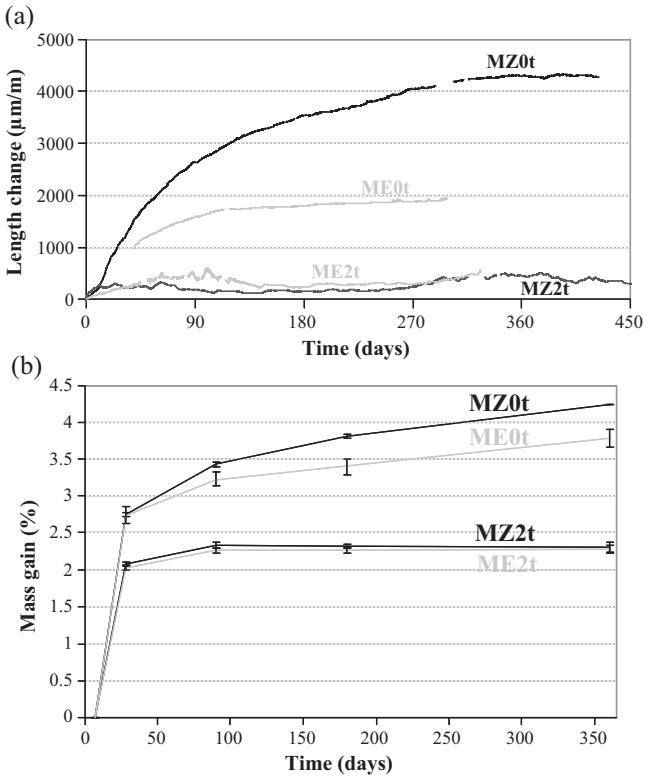

Fig. 13. Length change (a) and mass gain (b) of 4 cm × 4 cm × 16 cm mortar specimens submitted to a thermal treatment at early age, and subsequently cured under water.

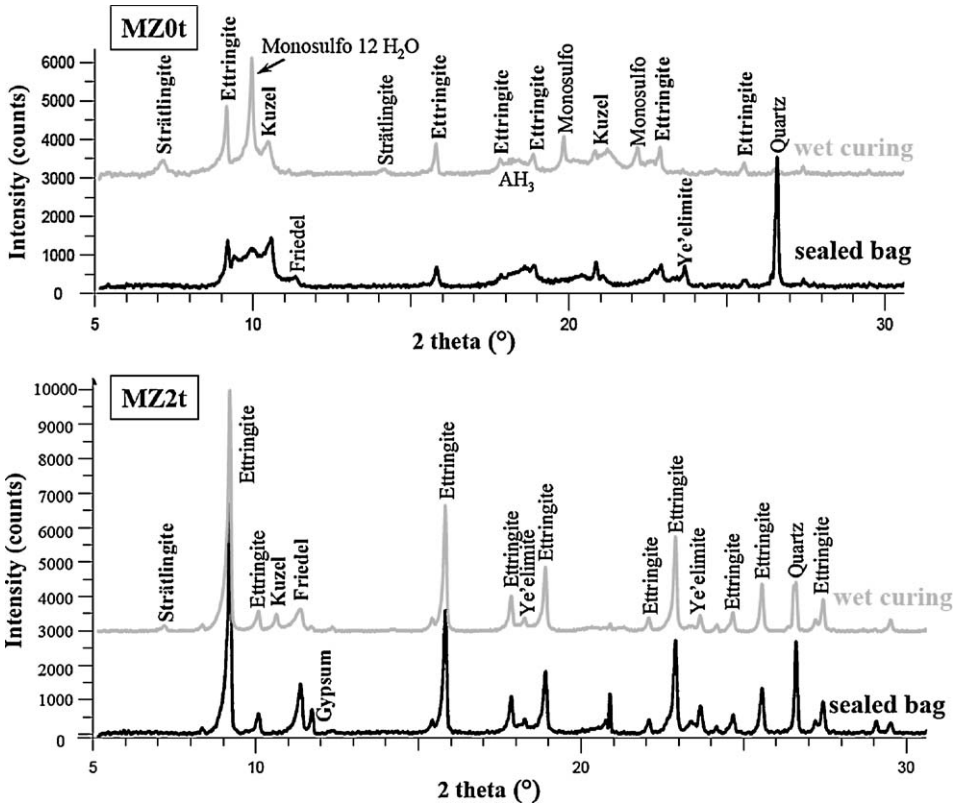

Fig. 14. X-ray diffraction patterns of one-year old mortars MZ0t and MZ2t cured under water or in sealed bag.

during the first 28 d and tended to stabilize after 90 d for samples ME2t and MZ2t, but not for the gypsum-free mortars which also exhibited higher water uptake.

Swelling under water was also highly dependent on the initial gypsum content of the binder and on the $ZnCl_2$ concentration in the mixing solution. Mortar MZ2t exhibited the same behaviour as reference ME2t, with a small length change which remained below 400 μm/m after one year. On the contrary, the expansion of mortar MZ0t (+4100 μm/m at 1 year) was almost twice that of mortar ME0t (+2000 μm/m), which was itself characterized by high swelling compared with gypsum-containing materials. This significant expansion did not induce any cracking of the samples at the macroscopic scale. However, the wet curing decreased the compressive strength of mortar MZ0t (24 MPa) by 42% and increased its water porosity (15.8 ± 0.2%) by 12% compared with curing in a sealed bag.

In order to understand the origin of the volume instability of gypsum-free materials, one-year-old mortars MZ0t and MZ2t were characterized by X-ray diffraction after their curing under water, and their mineralogy was compared to similar samples cured in sealed bags (Fig. 14). Mortar MZ0t exhibited significant mineralogical changes: under wet curing, precipitation of strätlingite, ettringite and monosulfoaluminate was observed, whereas the amount of chloro-AFm phases (Friedel's and Kuzel's salt) tended to decrease. This could result from the continuation of hydration, but also from the leaching of chlorides. Their concentration in the curing solution (750 mL for a 4 cm × 4 cm × 16 cm specimen) after one year reached indeed 19 mmol/L. Three main processes could contribute to the volume change:

- the retarded ettringite formation, due to the restart of hydration and/or to the reprecipitation of primary ettringite decomposed by the thermal excursion,
- the precipitation of strätlingite from C_2S and AH_3 ($\Delta V/V$ = +3.5%),
- the transformation of chloro-AFm phases into monosulfoaluminate, the Friedel's salt (268 mL/mol) and Kuzel's salt (289 mL/mol) having a smaller molar volume than monosulfoaluminate (309 mL/mol).

By contrast, the mineralogy of sample MZ2t was less dependent on the curing conditions. The ongoing hydration induced by wet curing led to the precipitation of small amounts of strätlingite and Kuzel's salt, while Friedel's salt was partly depleted. The amount of ettringite did not exhibit noticeable variations. The leaching of chlorides was reduced (11 mmol/L in the curing solution). Under wet curing, the porosity of mortar MZ2t (12.2 ± 0.2%) decreased by 10%, and its compressive strength (53 MPa) slightly increased (by 8%), as compared with curing in a sealed bag.

3.5. Zinc confinement by the cement matrix

The CSA cement matrix provided very good Zn^{2+} confinement, whatever its gypsum content.

(i) The zinc concentration in the pore solution extracted from paste CZ2t aged of 1 d, 7 d and 28 d always remained below the detection limit of the analytical method (2 μmol/L).
(ii) Mortars MZ0t and MZ2t were cured under water for one year to investigate their volume stability. At the end of the experiments, the solutions were analysed and were found free of zinc.

4. Conclusion

The purpose of this work was to assess the potential of CSA cements for $ZnCl_2$ stabilization/solidification. The main conclusions can be summarized as follows.

1. CSA cements were interesting candidates. Their setting was never inhibited, even at high $ZnCl_2$ (0.5 mol/L) in the mixing water, and zinc was readily insolubilized. Blending the CSA clinker with 20% gypsum was recommended for several reasons. (i) The hydration delay observed for a gypsum-free binder was suppressed. The strong retardation caused by chloride anions was indeed offset by the cumulative accelerating effects of zinc and sulfate ions. (ii) The temperature rise and cumulative heat produced during hydration were reduced. (iii) The compressive strength of the hardened materials was improved and their expansion under wet curing strongly limited. (iv) Their mineralogy was less dependent on the thermal history at early age.
2. When the CSA cements were hydrated with a $ZnCl_2$ solution, chloro-AFm precipitated. Fully hydrated materials contained ettringite, amorphous aluminum hydroxide, strätlingite and Kuzel's salt irrespective of the gypsum content. In addition, monosulfoaluminate was detected when a gypsum-free cement was used, while Friedel's salt precipitated when the cement initially contained 20% gypsum. Transient phases also formed with ongoing hydration: an unidentified compound named phase λ and gypsum (binders with 0% or 20% gypsum), together with Friedel's salt and CAH_{10} (binder with 0% gypsum). The latter was however only observed when hydration occurred at ambient temperature.
3. Hydration of CSA cement is more exothermic than that of OPC. Since a significant amount of heat is released within the first 12 h, large-volume drums of cemented waste forms may exhibit substantial temperature rise. With CSA cements, it is most important, for laboratory studies on small scale samples, to take into account this thermal evolution at early age in order to understand how actual cemented waste forms will perform. Applying a cycle reproducing the temperature rise (up to 80–85 °C) and fall in a massive mortar block accelerated the rate of hydration of the cement–waste grout, especially in the absence of gypsum. Moreover, the hydrate assemblage was modified. When gypsum-free cement was used, high temperatures promoted the precipitation of monosulfoaluminate instead of ettringite, and CAH_{10} was no longer formed. When the cement contained 20% gypsum, the mineralogy was less dependent on the curing conditions and only minor evolutions were observed (increased precipitation of Friedel's salt, slight decrease in the ettringite content).

Future work will be focussed on the behaviour under leaching of a $ZnCl_2$-rich waste stabilized with CSA cement, with two main objectives:

- assess the degradation rates and the mineralogical evolutions involved,
- determine the mechanisms of zinc retention by the solid matrix, and the nature of phase λ formed at early age.

References

[1] L. Cecille, C. Kertesz (Eds.), Treatment and Conditioning of Radioactive Incinerator Ashes, Elsevier Science Publishers Ltd, London, 1991, p. 239.
[2] G. Arliguie, J. Grandet, Etude par calorimétrie de l'hydratation du ciment Portland en présence de zinc, Cem. Concr. Res. 15 (1985) 825–832.
[3] G. Arliguie, J. Grandet, Study of cement hydration in presence of zinc – influence of gypsum content, Cem. Concr. Res. 20 (1990) 346–354.
[4] J. Dale Ortego, S. Jackson, G.S. Yu, H. McWhinney, D.L. Cocke, Solidification of hazardous substances – a TGA and FTIR study of Portland cement containing metal nitrates, J. Environ. Sci. Health A 24 (1989) 589–602.
[5] M.J. Cullinane Jr., R.M. Bricka, N.R. Francingues Jr., An Assessment of Materials That Interfere with Stabilization/Solidification Processes, Report EPA/600/9-87/015, Environmental Protection Agency, WA, 1987, pp. 64–71.
[6] I. Fernandez Olmo, E. Chacon, A. Irabien, Influence of lead, zinc, iron(III) and chromium(III) oxides on the setting time and strength development of Portland cement, Cem. Concr. Res. 31 (2001) 1213–1219.
[7] I.W. Hamilton, N.M. Sammes, Encapsulation of steel foundry dusts in cement mortar, Cem. Concr. Res. 29 (1999) 55–61.
[8] P.A. Spear, Zinc in Aquatic Environment: Chemistry, Distribution and Toxicology, National Research Council of Canada, Environmental Secretariat Publication 17589, Publications NRCC/CNRC, Ottawa, 1981.
[9] R.A. Goyer, Toxic effect of metals, in: M.O. Amdur, J. Doull, C.D. Klassen (Eds.), Casarett and Doull's Toxicology, The Basic Science of Poisons, Permagon Press, New York, 1991, p. 1032.
[10] F. Ziegler, R. Giere, C.A. Johnson, Sorption mechanisms of zinc to calcium silicate hydrate: sorption and microscopic investigations, Environ. Sci. Technol. 35 (2001) 4556–4561.
[11] I. Moulin, W.E.E. Stone, J. Sanz, J.Y. Bottero, F. Mosnier, C. Haehnel, Lead and zinc retention during hydration of tri-calcium silicate, a study by sorption isotherms and ^{29}Si NMR spectroscopy, Langmuir 15 (1999) 2829–2835.
[12] S. Komarneni, E. Breval, D.M. Roy, R. Roy, Reactions of some calcium silicates with metal cations, Cem. Concr. Res. 18 (1988) 204–220.
[13] F. Ziegler, A.M. Sheidegger, C.A. Johnson, R. Dähn, E. Wieland, Sorption mechanisms of zinc to calcium silicate hydrate: X-ray absorption fine structure (XAFS) investigation, Environ. Sci. Technol. 35 (2001) 1550–1555.
[14] A. Stumm, K. Garbev, G. Beuchle, L. Black, P. Stemmermann, R. Nüesch, Incorporation of zinc into calcium silicate hydrates – part I – formation of C–S–H (I) with C/S = 2/3 and its isochemical counterpart gyrolite, Cem. Concr. Res. 35 (2005) 1665–1675.
[15] G. Arliguie, J.P. Ollivier, J. Grandet, Etude de l'effet retardateur du zinc sur l'hydratation de la pâte de ciment Portland, Cem. Concr. Res. 12 (1982) 79–86.
[16] G. Arliguie, J. Grandet, Influence de la composition d'un ciment Portland sur son hydratation en présence de zinc, Cem. Concr. Res. 20 (1990) 517–524.
[17] J. Dale Ortego, Y. Barroeta, F.K. Cartledge, H. Akhter, Leaching effects on silicate polymerization – an FTIR and 29Si NMR study of lead and zinc in Portland cement, Environ. Sci. Technol. 25 (1991) 1171–1174.
[18] M. Yousuf, A. Mollah, K. Vempati, T.C. Lin, D.L. Cocke, The interfacial chemistry of solidification/stabilization of metals in cement and pozzolanic materials systems, Waste Manage. 15 (1995) 137–148.
[19] S. Asavapisit, G. Fowler, C.R. Cheeseman, Solution chemistry during cement hydration in the presence of metal hydroxide wastes, Cem. Concr. Res. 27 (8) (1997) 1249–1260.
[20] C.S. Poon, A.J. Clark, C.J. Peters, R. Perry, Mechanisms of metal fixation and leaching by cement-based fixation processes, Waste Manage. 3 (1985) 127–142.
[21] M. Drouin, Enrobage de déchets Melox pauvres en plutonium dans une matrice de liants hydrauliques, Mémoire CNAM, 1994.
[22] A. Klein, G.E. Troxell, Studies of calcium sulfoaluminate admixture for expansive cements, in: ASTM Proceedings, 1958, p. 986.
[23] R.K. Mehta, Investigation on the products in the system C_4A_3S–$CaSO_4$–CaO–H_2O, in: Annual Meeting of the Highway Research Board Proceedings, 1965, pp. 328–352.
[24] I. Odler, Special inorganic cements, in: A. Bentur, S. Mindness (Eds.), Modern Concrete Technology, vol. 8, E&F.N. Son, London, 2000, pp. 69–87.
[25] T. Sui, Y. Yao, Recent progress in special cements in China, in: Proc. 11th International Conference on the Chemistry of Cement, Durban, South Africa, 11–16 May, 2003, pp. 2028–2032.
[26] O. Andac, F.P. Glasser, Microstructure and microchemistry of calcium sulfoaluminate cement, Mater. Res. Soc. Symp. Proc. 370 (1995) 132–142.
[27] F.P. Glasser, L. Zhang, High performance cement matrices based on calcium sulfoaluminate-belite compositions, Cem. Concr. Res. 31 (2001) 1881–1886.
[28] L. Zhang, F.P. Glasser, Hydration of calcium sulfoaluminate cement at less than 24 h, Adv. Cem. Res. 14 (2002) 141–155.
[29] V. Kasselouri, P. Tsakiridis, C. Malami, B. Georgali, C. Alexandridou, A study on the hydration products of a non-expansive sulfoaluminate cement, Cem. Concr. Res. 25 (1995) 1726–1736.
[30] F. Winnefeld, S. Barlag, Calorimetric and thermogravimetric study on the influence of calcium sulfate on the hydration of ye'elimite, J. Therm. Anal. Calorim. 101 (2010) 949–957.
[31] F.P. Glasser, L. Zhang, Calculation of chemical water demand for hydration of calcium sulfoaluminate cement, in: Proceedings of the 4th International Symposium on Cement and Concrete, Shanghai, 1998, pp. 38–44.
[32] F.P. Glasser, L. Zhang, Q. Zhou, Reactions of aluminate cements with calcium sulfate, in: Proceedings of the International Conference on Calcium Aluminate Cements, Edinburgh, Scotland, 2001, pp. 551–564.
[33] M. Andac, F.P. Glasser, Pore solution composition of calcium sulfoaluminate cement, Adv. Cem. Res. 11 (1999) 23–26.
[34] F. Winnefeld, B. Lothenbach, Hydration of calcium sulfoaluminate cements – experimental findings and thermodynamic modelling, Cem. Concr. Res. 40 (2010) 1239–1247.
[35] M.C. Martin-Sedeno, A.J.M. Cuberos, A.G. dela Torre, G. Alvarez-Pinazo, L.M. Ordonez, M. Gateshki, M.A.G. Aranda, Aluminum-rich belite sulfoaluminate cements: clinkering and early age hydration, Cem. Concr. Res. 40 (2010) 359–369.
[36] L. Zhang, F.P. Glasser, Investigation of the microstructure and carbonation of CSA-based concretes removed from service, Cem. Concr. Res. 35 (2005) 2252–2260.
[37] S. Berger, C. Cau Dit Coumes, P. Le Bescop, D. Damidot, Hydration of calcium sulfoaluminate cement by a $ZnCl_2$ solution: investigation at early age, Cem. Concr. Res. 30 (2009) 1180–1187.
[38] V. Albino, R. Cioffi, M. Marroccoli, L. Santoro, Potential application of ettringite generating systems for hazardous waste stabilization, J. Hazard. Mater. 51 (1996) 241–252.

[39] R. Berardi, R. Cioffi, L. Santoro, Matrix stability and leaching behaviour in ettringite-based stabilization systems doped with heavy metals, Waste Manage. 17 (1997) 535–540.
[40] J. Pera, J. Ambroise, M. Chabannet, Valorization of automotive shredder residue in building materials, Cem. Concr. Res. 34 (2004) 557–562.
[41] S. Peysson, J. Pera, M. Chabannet, Immobilization of heavy metals by calcium sulfoaluminate cement, Cem. Concr. Res. 35 (2005) 2261–2270.
[42] M.L.D. Gougar, B.E. Scheetz, D.M. Roy, Ettringite and C–S–H Portland cement phases for waste immobilization: a review, Waste Manage. 16 (1996) 295–303.
[43] G.J. Mc Carthy, D.J. Hassett, J.A. Bender, Synthesis, crystal chemistry and stability of ettringite, a material with potential applications in hazardous waste immobilization, Mater. Res. Soc. Symp. Proc. 245 (1992) 129–140.
[44] S. Auer, H.J. Kuzel, H. Pollmann, F. Sorrentino, Investigation on MSW fly ash treatment by reactive calcium aluminates and phases formed, Cem. Concr. Res. 25 (1995) 1347–1359.
[45] P. Benard, C. Cau Dit Coumes, S. Garrault, A. Nonat, S. Courtois, Dimensional stability under wet curing of mortars containing high amounts of nitrates and phosphates, Cem. Concr. Res. 38 (2008) 1181–1189.
[46] J. Van der Lee, Thermodynamic and Mathematical Concepts of CHESS. Technical Report LHM/RD/98/39, 1998, 99 pp.
[47] S. Berger, C. Cau Dit Coumes, P. Le Bescop, D. Damidot, Physico-chemical evolution of calcium sulfoaluminate cements with variable gypsum contents during hydration. Influence of a thermal excursion at early age, Cem. Concr. Res. 41 (2011) 149–160.
[48] M. Balonis, B. Lothenbach, G. Le Saout, F.P. Glasser, Impact of chloride on the mineralogy of hydrated Portland cement systems, Cem. Concr. Res. 40 (2010) 1009–1022.
[49] S. Peysson, Contribution à l'Etude de la Stabilisation de Déchets par du Ciment Sulfo-alumineux, PhD thesis, INSA Lyon, France, 2005.
[50] D. Damidot, F.P. Glasser, Thermodynamic Investigation of the $CaO–Al_2O_3–CaSO_4–H_2O$ system at 50 °C and 85 °C, Cem. Concr. Res. 22 (1992) 1179–1191.
[51] F.P. Glasser, A. Kindness, S.A. Stronach, Stability and solubility relationships in AFm phases: part I. Chloride, sulfate and hydroxide, Cem. Concr. Res. 29 (1999) 861–866.
[52] J.D. Allison, D.S. Brown, K.J. Novo-Gradac, MINTEQA2/PRODEF2, A Geochemical Assessment Model for Environmental Systems: Version 3.0 User's Manual, EPA/600/3-91/021, EPA, Athens, GA, USA, 1991.
[53] F. Ziegler, C.A. Johnson, The solubility of calcium zincate ($CaZn_2(OH)_6{\cdot}2H_2O$), Cem. Concr. Res. 31 (2001) 1327–1332.